The J-domain cochaperone Rsp1 interacts with Mto1 to organize noncentrosomal microtubule assembly

Juan Shen[a,b,c,†], Tianpeng Li[a,b,c,†], Xiaojia Niu[a,b,c,†], Wenyue Liu[a,b,c], Shengnan Zheng[a,b,c], Jing Wang[a,b,c], Fengsong Wang[d], Xinwang Cao[d], Xuebiao Yao[a,b,c], Fan Zheng[a,b,c,*], and Chuanhai Fu[a,b,c,*]

[a]Division of Molecular and Cell Biophysics, Hefei National Science Center for Physical Sciences, University of Science and Technology of China, Hefei, Anhui 230027, China; [b]Chinese Academy of Sciences Center for Excellence in Molecular Cell Sciences, School of Life Sciences, University of Science and Technology of China, Hefei, Anhui 230027, China; [c]Anhui Key Laboratory for Cellular Dynamics and Chemical Biology, University of Science and Technology of China, Hefei 230027, China; [d]School of Life Sciences, Anhui Medical University, Hefei, Anhui 230027, China

ABSTRACT **Microtubule biogenesis initiates at various intracellular sites, including the centrosome, the Golgi apparatus, the nuclear envelope, and preexisting microtubules. Similarly, in the fission yeast *Schizosaccharomyces pombe*, interphase microtubules are nucleated at the spindle pole body (SPB), the nuclear envelope, and preexisting microtubules, depending on Mto1 activity. Despite the essential role of Mto1 in promoting microtubule nucleation, how distribution of Mto1 in different sites is regulated has remained elusive. Here, we show that the J-domain cochaperone Rsp1 interacts with Mto1 and specifies the localization of Mto1 to non-SPB nucleation sites. The absence of Rsp1 abolishes the localization of Mto1 to non-SPB nucleation sites, with concomitant enrichment of Mto1 to the SPB and the nuclear envelope. In contrast, Rsp1 overexpression impairs the localization of Mto1 to all microtubule organization sites. These findings delineate a previously uncharacterized mechanism in which Rsp1-Mto1 interaction orchestrates non-SPB microtubule formation.**

Monitoring Editor
Thomas Surrey
The Francis Crick Institute

Received: May 8, 2018
Revised: Oct 30, 2018
Accepted: Nov 9, 2018

INTRODUCTION

Microtubules play crucial roles in a wide range of cellular activities, and microtubule nucleation is initiated at multiple intracellular sites in a cell type– and/or cell cycle–dependent manner (Xia *et al.*, 2014; Lin *et al.*, 2015; Petry and Vale, 2015; Roostalu and Surrey, 2017; Wu and Akhmanova, 2017). These multiple intracellular sites, termed microtubule-organizing centers (MTOCs), include the centrosome, the nuclear envelope, the Golgi apparatus, the cell cortex, and preexisting microtubules (Wu and Akhmanova, 2017). Generally, microtubule nucleation begins with recruitment of γ-TuRC (γ-tubulin ring complex), which comprises γ-tubulin and GCP2-6 (γ-tubulin complex proteins 2-6), to MTOCs (Lin *et al.*, 2015; Oakley *et al.*, 2015; Petry and Vale, 2015). The CM1 (centrosomin motif 1) motif-containing protein CDK5RAP2 (CDK5 regulatory subunit–associated protein 2) has been shown to be a key player in recruiting γ-TuRC to noncentrosomal MTOCs. Additionally, CDK5RAP2 functions to activate γ-TuRC–mediated microtubule nucleation (Fong *et al.*, 2008; Choi *et al.*, 2010; Hanafusa *et al.*, 2015). The homologues or the functional counterparts of CDK5RAP2 have been identified and functionally characterized in *Caenorhabditis elegans* (Hamill *et al.*, 2002; Woodruff *et al.*, 2017), *Drosophila melanogaster* (Terada *et al.*, 2003), *Saccharomyces cerevisiae* (Knop and Schiebel, 1998; Usui *et al.*, 2003), and *Schizosaccharomyces pombe* (Sawin *et al.*, 2004; Anders *et al.*, 2006).

The fission yeast *Schizosaccharomyces pombe* has been an excellent model organism for the study of microtubules due to the simplicity of its microtubule organization (Hagan and Hyams, 1988; Hagan, 1998). Interphase fission yeast cells contain 2–6 microtubule

This article was published online ahead of print in MBoC in Press (http://www.molbiolcell.org/cgi/doi/10.1091/mbc.E18-05-0279) on November 14, 2018.

†These authors contributed equally.

Author contributions: C.F. conceived the project. J.S., T.L., X.N., W.L., S.Z., and J.W. performed the experiments. J.S., T.L., F.Z., and C.F. analyzed the data. X.Y., F.Z., and C.F. wrote the paper. All authors made comments.

*Address correspondence to: Chuanhai Fu (chuanhai@ustc.edu.cn) or Fan Zheng (zhengfan@ustc.edu.cn).

Abbreviations: γ-TuRC, γ-tubulin ring complex; γ-TuSC, γ-tubulin small complex; CDK5RAP2, CDK5 regulatory subunit–associated protein 2; CM1, centrosomin motif 1; Cut11, red fluorescent protein; DDO, double-dropout; eMTOC, equatorial MTOC; GCP, γ-tubulin complex protein; GFP, green fluorescent protein; GST, glutathione *S*-transferase; iMTOC, interphase MTOC; MTOC, microtubule-organizing center; PAA, postanaphase microtubule array; QDO, quadruple-dropout; SPB, spindle pole body; WT, wild type; YE, yeast extract.

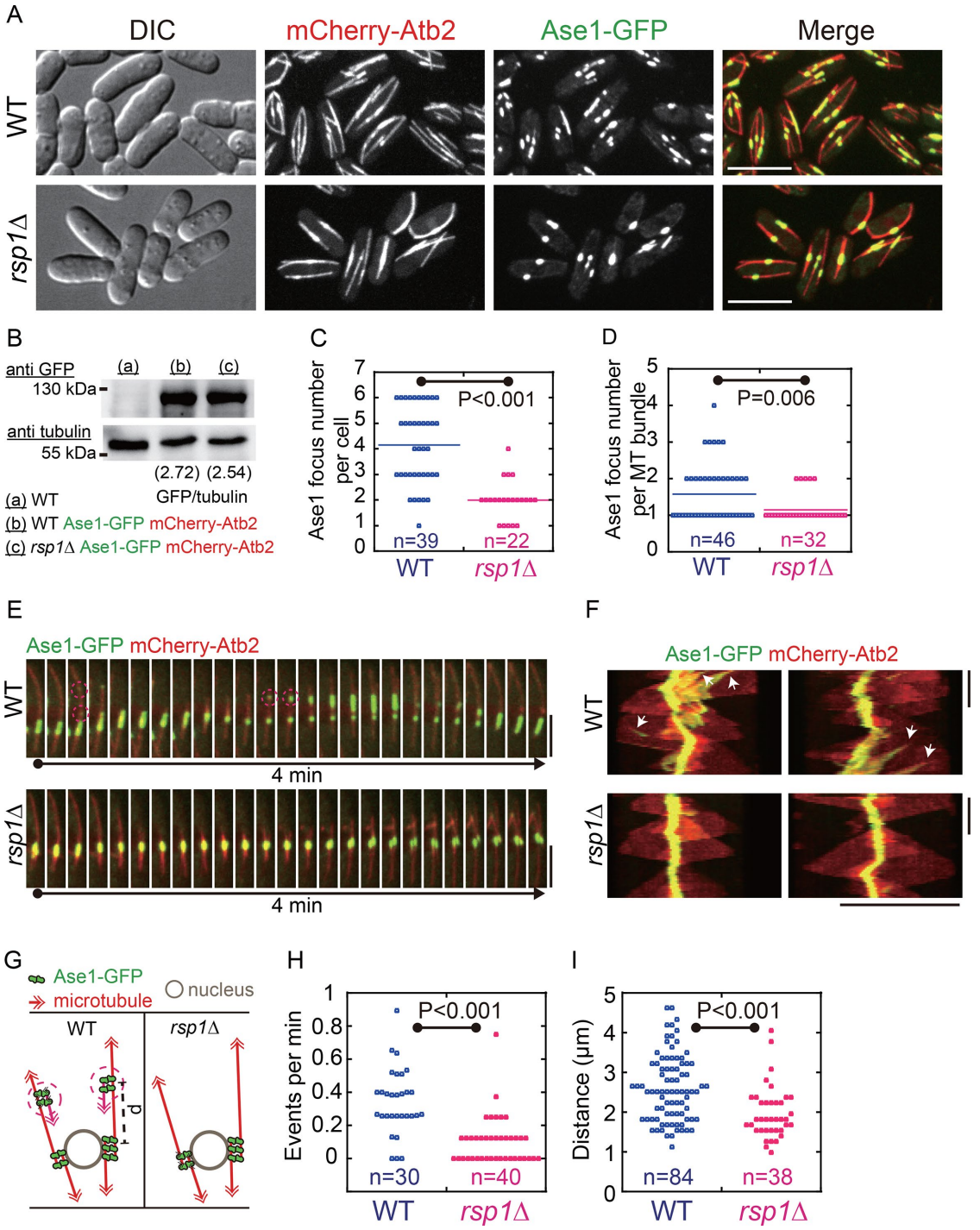

FIGURE 1: The absence of Rsp1 impairs formation of non-SPB microtubules on preexisting microtubules. (A) Maximum projection images of WT and rsp1-deletion (*rsp1*Δ) cells expressing Ase1-GFP (a microtubule bundler) and mCherry-Atb2 (α-tubulin). Note that most of the *rsp1*Δ cells displayed 1–2 Ase1-GFP foci adjacent to the nucleus, whereas WT cells displayed dispersed Ase1-GFP along microtubules, with some Ase1 displaying as bar structures around the middle of the cells. DIC indicates differential interference contrast. Scale bar: 10 μm. (B) Western blot analysis of Ase1-GFP expression in the indicated cells (a–c). Antibodies against GFP and tubulin were used. See the full membranes in Supplemental Figure S1. The ratio of GFP/tubulin intensity is shown in parentheses. (C) Quantification of Ase1 focus number per cell for WT and *rsp1*Δ cells. The *p* value was calculated by Wilcoxon–Mann–Whitney test, and *n* indicates cell number. (D) Quantification of Ase1 focus number per microtubule bundle for WT and *rsp1*Δ cells. The *p* value was calculated by Wilcoxon–Mann–Whitney test, and *n* indicates MT bundle number. (E) Maximum projection time-lapse images of WT and *rsp1*Δ cells expressing Ase1-GFP and mCherry-Atb2. Note that a new microtubule (marked by the dashed circles) emerged on a preexisting microtubule and elongated toward the central microtubule overlapping region. In the absence of Rsp1, Ase1 residing at the central microtubule region appeared to be stably maintained. Scale bar: 5 μm. (F) Kymograph analysis of microtubule and Ase1-GFP dynamics in WT and *rsp1*Δ cells. Newly generated

bundles arranged in an antiparallel configuration within the cytoplasm (Drummond and Cross, 2000; Sagolla *et al.*, 2003; Sawin and Tran, 2006; Bratman and Chang, 2008). Within the bundles, four to five microtubules with mixed polarity are present (Hoog *et al.*, 2007). The evolutionarily conserved microtubule bundling protein Ase1 is a key player in mediating formation of the antiparallel microtubules (Loiodice *et al.*, 2005; Yamashita *et al.*, 2005; Janson *et al.*, 2007). Microtubule nucleation in fission yeast resembles that of higher eukaryotic cells, taking place at multiple MTOCs, including the SPB (spindle pole body, the counterpart of the centrosome), the equatorial MTOC (eMTOC) at the constriction ring region during late anaphase, the nuclear envelope (the interphase MTOC [iMTOC]), and preexisting microtubules (iMTOC) (Horio *et al.*, 1991; Sawin and Tran, 2006; Lin *et al.*, 2015). Similarly, fission yeast possesses γ-tubulin and GCP2-6. GCP2 (Alp4), GCP3 (Alp6), and γ-tubulin (Gtb1) initially form the complex of γ-TuSC (γ-tubulin small complex) and then γ-TuRC by associating with GCP4 (Gfh1), GCP5 (Mod21), and GCP6 (Alp16) (Fujita *et al.*, 2002; Anders *et al.*, 2006; Lin *et al.*, 2015). Recently, Mzt1, the fission yeast homologue of MORZART (GCP7-8), was added to the expanding GCP protein list and was reported to be required, but not sufficient, for recruiting γ-TuRC to the SPB (Dhani *et al.*, 2013; Masuda *et al.*, 2013).

In contrast to Mzt1, the fission yeast CDK5RAP2 homologue Mto1 is essential for recruiting γ-TuRC to the multiple non-SPB MTOCs, where it functions to activate γ-TuRC (Sawin *et al.*, 2004; Lynch *et al.*, 2014). The C-terminal MASC (Mto1 and Spc72 C terminus) region of Mto1 is responsible for targeting Mto1 to the SPB and eMTOC, while the N-terminal CM1 motif interacts with γ-TuRC (Samejima *et al.*, 2008, 2010). Moreover, Mto1 forms higher-order complexes with Mto2 to activate γ-TuRC–dependent microtubule nucleation (Lynch *et al.*, 2014). Owing to the limited availability of free Mto1 (Lynch *et al.*, 2014), Mto1 must be redistributed at multiple MTOCs to promote new microtubule nucleation. How such redistribution is regulated remains unknown.

The J-domain cochaperone Rsp1 has been demonstrated to be a key player in promoting disassembly of the postanaphase microtubule array (PAA) emanating from eMTOCs during cytokinesis (Zimmerman *et al.*, 2004). PAA disassembly is important for proper localization of Alp4/GCP2, the γ-TuRC component, to preexisting microtubules in the cytoplasm (Zimmerman *et al.*, 2004). Intriguingly, PAA formation depends on Mto1 (Sawin *et al.*, 2004; Zimmerman and Chang, 2005). These highly relevant findings prompted us to ask whether Rsp1 could promote Mto1 redistribution at the multiple iMTOCs to organize microtubule assembly. We found that Rsp1 physically interacts with Mto1 and that the interaction is required for organizing noncentrosomal microtubules within the cell.

RESULTS

Rsp1 is required for non-SPB microtubule formation on preexisting microtubules

It has been reported that the absence of Rsp1 impairs interphase microtubule organization (Zimmerman *et al.*, 2004). To revisit the microtubule phenotype, we examined wild-type (WT) and *rsp1*Δ cells expressing Ase1-GFP (Ase1–green fluorescent protein) (microtubule bundling factor) and mCherry-Atb2 (α-tubulin) by live-cell microscopy at 5-s intervals. As shown in Figure 1A, Ase1 in WT cells dispersed on microtubule bundles either as bar or dot structures with various sizes, indicative of formation of complex microtubule arrays within the bundles. By contrast, Ase1 in most of the *rsp1*Δ cells concentrated as 1- to 2-dot structures on microtubules, indicative of defective microtubule organization within microtubule bundles (Figure 1, C and D). Such defective microtubule organization was not due to altered expression of Ase1, because the expression levels of Ase1 in WT and *rsp1*Δ cells were comparable (Figure 1B). Furthermore, time-lapse microscopic analysis showed that newly formed non-SPB microtubules (marked by Ase1-GFP) were clearly visible on preexisting microtubules in WT cells, but not in *rsp1*Δ cells (Figure 1, E–G). Intriguingly, the size and the positioning of the microtubule overlapping regions marked by Ase1-GFP were apparently more stable in *rsp1*Δ cells than in WT cells. We then sought to quantify the occurrence frequency of the non-SPB microtubules and the distance between the non-SPB microtubule nucleation site and the medial microtubule overlapping region marked by Ase1-GFP (Figure 1G). The occurrence frequency of the non-SPB microtubule assembly decreased significantly in *rsp1*Δ cells, with the majority of the *rsp1*Δ cells displaying no or few newly formed non-SPB microtubules (Figure 1H). These quantification data confirmed that the absence of Rsp1 impairs the formation of non-SPB microtubules within microtubule bundles. In some *rsp1*Δ cells, non-SPB microtubule assembly was initiated at a low frequency, and such non-SPB microtubules appeared to be positioned closer to the medial microtubule overlapping region than those of WT cells (Figure 1I). Thus, we concluded that Rsp1 is a key player in regulating the formation of non-SPB microtubules using preexisting microtubules.

The localization of Mto1 to preexisting microtubules requires Rsp1

We reasoned that the defective formation of non-SPB microtubules in *rsp1*Δ cells could be caused by Mto1 malfunctions, because Mto1 localizes to all iMTOCs and is the key player in promoting microtubule nucleation (Sawin *et al.*, 2004). To test this possibility, we examined the localization of Mto1, as well as its associated protein Mto2, which is required for the formation of Mto1 and Mto2 higher-order structures, and the γ-TuRC component Alp4, by live-cell microscopy. In WT cells, Mto1 appeared as many particles on microtubule bundles (Figure 2, A and C). By contrast, the number of Mto1 particles was drastically reduced in *rsp1*Δ cells (Figure 2, A and C), and intriguingly, the remaining few Mto1 particles were significantly larger than those of WT cells (Figure 2D), indicative of Mto1 accumulation. This was confirmed by measurements of the average fluorescence intensity of each Mto1 focus (Figure 2E). The dramatic change of Mto1 in localization likely was not caused by altered protein expression, because the protein levels of Mto1 in WT and *rsp1*Δ cells were comparable (Figure 2B). Similar phenotypes were observed for

microtubules on preexisting microtubules (indicated by white arrows) were often detected in WT cells but not in *rsp1*Δ cells. Note that while the central microtubule overlapping regions in WT cells are dynamic, the ones in *rsp1*Δ cells are stably maintained. Scale bars at the bottom and on the right represent 5 μm and 2 min, respectively. (G–I) Diagrams illustrating new microtubule generation (indicated by dashed circles) on preexisting microtubules in WT and *rsp1*Δ cells (G). The frequency of newly generated microtubules on preexisting microtubules is shown in H. The "d" in the diagram indicates the distance of a newly generated microtubule from the central microtubule overlapping region, and the corresponding quantification is shown in I. Note that both the frequency and the distance are significantly decreased in *rsp1*Δ cells. The *p* values were calculated by Student's *t* test, and *n* indicates microtubule bundle number.

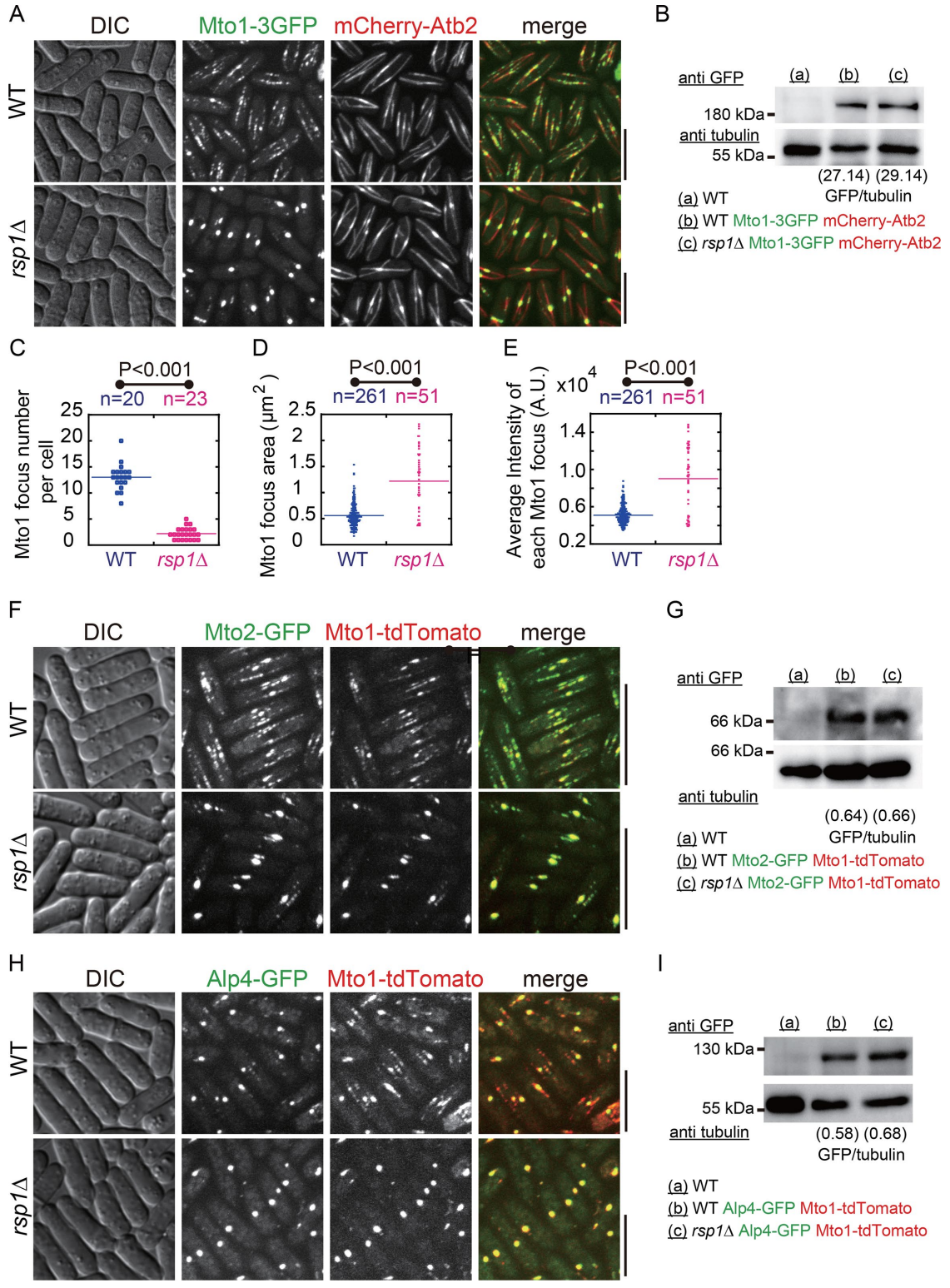

FIGURE 2: The absence of Rsp1 abolishes the localization of Mto1, Mto2, and Alp4 to microtubules. (A) Maximum projection images of WT and *rsp1*Δ cells expressing Mto1-3GFP and mCherry-Atb2. Note that Mto1 localized along microtubules as many dots in WT cells, whereas in *rsp1*Δ cells, Mto1 became concentrated at the presumable SPB and/or the iMTOCs on the nuclear envelope (also see Supplemental Figure S2D for colocalization of Mto1 and Cut11-RFP [the nuclear envelope marker]). Scale bar: 10 μm. (B) Western blot analysis of Mto1-3GFP expression in the indicated cells (a–c). Antibodies against GFP and tubulin were used. See the full membranes in Supplemental Figure S2A. The ratio of GFP/tubulin intensity is shown in parentheses. (C) Quantification of Mto1 focus number per cell for WT and *rsp1*Δ cells. The *p* value was calculated by Wilcoxon–Mann–Whitney test, and *n* indicates cell number. (D) Dot plot of Mto1 focus area for WT and *rsp1*Δ cells. The *p* value was calculated by Student's *t* test, and *n* indicates focus number. (E) Dot plot of the average intensity of each Mto1 focus in WT and *rsp1*Δ cells. The *p* value was calculated by

Mto2 and Alp4, despite the fact that fewer Alp4 particles were present on microtubule bundles than Mto1 and Mto2 particles, even in WT cells (Figure 2, F–I, and Supplemental Figure S2, E–J). This is consistent with the notion that Mto1 particles on microtubules are capable of recruiting γ-TuRC components for promoting microtubule nucleation, though possibly not simultaneously (Sawin *et al.*, 2004). To reveal the precise localization of the enlarged Mto1 foci in *rsp1*Δ cells, we further imaged Mto1-3GFP in cells expressing Cut11-RFP (Cut11–red fluorescent protein; a protein localizing at the nuclear envelope and concentrating at the SPB) and mCherry-Atb2 before and after microtubule depolymerization by the drug methyl benzimidazol-2-yl-carbamate. As shown in Supplemental Figure S2D, the enlarged Mto1 foci in *rsp1*Δ cells clearly localized to the SPB and the nuclear envelope, presumably at the iMTOCs on the nuclear envelope. Hence, Rsp1 is required for the proper localization of Mto1, Mto2, and Alp4 on microtubule bundles.

Rsp1 prevents Mto1 accumulation

Microtubules are nucleated at the SPB and the non-SPB iMTOCs on the nuclear envelope and preexisting microtubules in interphase fission yeast cells (Sawin and Tran, 2006). These multiple intracellular nucleation sites complicated our dissection of the effect of Rsp1 on Mto1. To reduce the complexity of the analysis, we sought to focus our effort on analyzing Mto1 in anucleate cells, which do not have the SPB and the nuclear envelope iMTOCs. Most of the WT and *rsp1*Δ anucleate cells contained microtubules (Figure 3, A and B). Notably, the absence of Rsp1 in anucleate cells also led to abnormal accumulation of Mto1 in the middle of short and dense microtubules and Mto1 accumulation was distinct from that seen in the anucleate WT cells, in which small, scattered Mto1 particles decorated long microtubules (Figure 3, A, C, and D). In addition, the enlarged Mto1 foci in *rsp1*Δ cells displayed higher average fluorescence intensity (Figure 3E), suggesting Mto1 accumulation in the absence of Rsp1. Therefore, we concluded that Rsp1 is required to prevent excessive accumulation of Mto1.

Rsp1 colocalizes with Mto1 on microtubules

We then assessed the endogenous colocalization of Rsp1 and Mto1. Rsp1 is expressed at a very low level (see Figure 6, A and B, later in this article), making it challenging to observe endogenously, and previous work had to ectopically express Rsp1 at a moderate level for analyzing Rsp1 localization (Zimmerman *et al.*, 2004). We overcame this challenge by using mNeonGreen, a fluorescent protein ~3 times brighter than GFP (Shaner *et al.*, 2013). Rsp1 was fused to a tandem mNeonGreen tag and expressed at its own locus. This significantly improved Rsp1 signals (Figure 4A). In agreement with the previous data obtained by ectopic expression of Rsp1, endogenous Rsp1 localized both to microtubule plus ends and as scattering particles on microtubules (Figure 4, A and B). Some, but not all, Rsp1 particles colocalized with Mto1 (Figure 4C). Live-cell microscopic analysis further revealed that the colocalized Rsp1 and Mto1 signals could disappear during the observation (Figure 4D). These results suggest a dynamic localization relationship between Rsp1 and Mto1.

Rsp1 physically interacts with Mto1

Next, we tested the physical interaction between Rsp1 and Mto1 using yeast two-hybrid assays. As shown in Figure 5A, two Rsp1 C-terminal regions (i.e., aa 290–396 and 487–494) were required for interaction with Mto1. To reduce the complexity of analyzing truncation mutants, we chose to use Rsp1(1-486) which lacked the 8 amino acids at the extreme C-terminus (i.e., 487–494) for further biochemical and functional characterization. First, GST (glutathione *S*-transferase) pull-down and coimmunoprecipitation assays confirmed that Rsp1(1-486) displayed compromised interaction with endogenous Mto1 (Figure 5, B–D). Second, microscopic analysis showed that Rsp1(1-486) displayed significantly fewer particles within a cell than its full-length version (Figure 5E). Furthermore, Rsp1(1-486) mainly localized to the SPB and/or to the iMTOCs on the nuclear envelope but with significantly decreased signals on microtubules (Figure 5, F and G, and Supplemental Figure S3D). Consistent with these findings, the defective localization of Rsp1 (1-486) significantly impaired the localization of Mto1 to microtubules, but not to the SPB and/or the iMTOCs on the nuclear envelope, which phenocopied *rsp1*Δ cells (Figure 5, G and H). Interestingly, the absence of Mto1 also compromised the localization of Rsp1 to microtubules, but not to the SPB (Figure 5, I and J). Taken together, these results led us to conclude that Rsp1 physically interacts with Mto1 and that the interaction is important for both proteins to localize to microtubule bundles.

Rsp1 overexpression compromises the localization of Mto1 to preexisting microtubules

What could be the role of the interaction between Rsp1 and Mto1? The absence of Rsp1 causes excessive accumulation of Mto1 at the SPB and/or at the iMTOCs on the nuclear envelope, compromising the microtubule localization of Mto1 (Figure 2). These phenotypes, together with the finding that Rsp1 localizes to microtubules in an Mto1 dependent manner (Figure 5), prompted us to hypothesize that Rsp1 may function through promoting Mto1 redistribution at MTOCs. If this is the case, Rsp1 overexpression should impair Mto1 localization to all MTOCs, because an excessive amount of Rsp1 will sustain the interaction between Rsp1 and Mto1 and abnormally destabilize Mto1 at MTOCs.

For testing the hypothesis, Rsp1 fused to GFP was expressed from endogenous, *ase1* (P_{ase1}), or *cam1* (P_{cam1}) promoter. Western blot analysis showed that the expression level of endogenous Rsp1 is much lower than the levels of ectopically expressed Rsp1 and that the strain with the *cam1* promoter has the highest expression level (Figure 6B). This was consistent with our observations under the

Student's *t* test, and *n* indicates focus number. (F) Maximum projection images of WT and *rsp1*Δ cells expressing Mto2-GFP and Mto1-tdTomato. Similar to Mto1, Mto2 was concentrated at the SPB and/or the iMTOCs on the nuclear envelope. See quantification of Mto2 focus number and measurements of Mto2 focus area and the average intensity of each Mto2 focus in Supplemental Figure S2, E and G. Scale bar: 10 μm. (G) Western blot analysis of Mto2-GFP expression in the indicated cells. See the full membranes in Supplemental Figure S2B. The ratio of GFP/tubulin intensity is shown in parentheses. (H) Maximum projection images of WT and *rsp1*Δ cells expressing Alp4-GFP and Mto1-tdTomato. Similarly, Alp4 was concentrated at the SPB and/or the iMTOCs on the nuclear envelope. See quantification of Alp4 focus number and measurements of Alp4 focus area and the average intensity of each Alp4 focus in Supplemental Figure S2, H–J. Scale bar: 10 μm. (I) Western blot analysis of Alp4-GFP expression in the indicated cells. See the full membranes in Supplemental Figure S2C. The ratio of GFP/tubulin intensity is shown in parentheses.

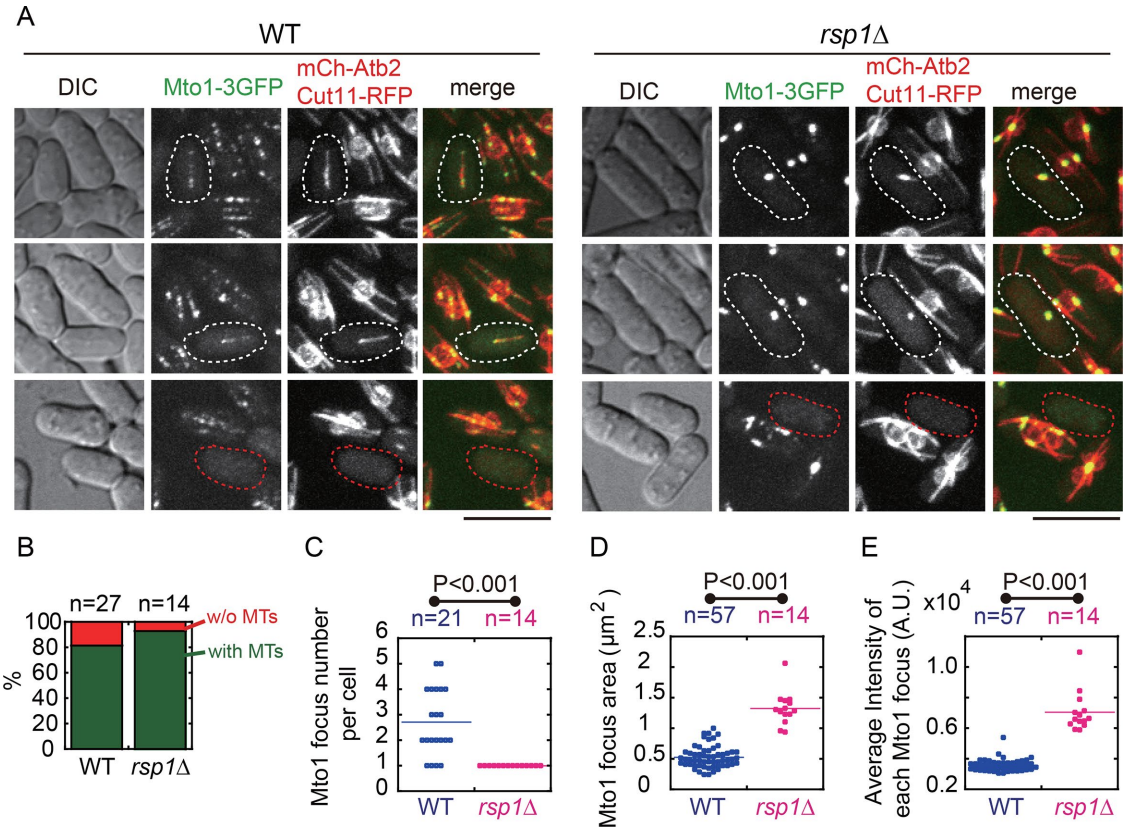

FIGURE 3: Mto1 localization in anucleate cells. (A) Maximum projection images of WT and *rsp1*Δ cells expressing Mto1-3GFP, mCherry-Atb2, and Cut11-RFP (the nuclear envelope marker). Cells without the nuclei were prepared by high-speed centrifugation (indicated by dashed lines). Note that the absence of Rsp1 caused Mto1 concentration independent of the SPB and the nuclear envelope. (B) Quantification of the nucleus-lacking WT and *rsp1*Δ cells bearing microtubules. *n* indicates cell number. (C) Quantification of Mto1 focus number per cell for WT and *rsp1*Δ anucleate cells. The *p* value was calculated by Wilcoxon–Mann–Whitney test, and *n* indicates cell number. (D) Dot plot of Mto1 focus area for WT and *rsp1*Δ cells. The *p* value was calculated by Student's *t* test, and *n* indicates focus number. (E) Dot plot of the average intensity of each Mto1 focus in WT and *rsp1*Δ cells. The *p* value was calculated by Student's *t* test, and *n* indicates focus number.

microscope (Figure 6A). The number of microtubule bundles decreased significantly as the expression levels of Rsp1 increased (Figure 6, A and C), consistent with the results derived from similar Rsp1 overexpression experiments (from the thiamine-repressible promoter nmt1), as reported previously (Zimmerman *et al.*, 2004). Intriguingly, we found that microtubules in cells expressing Rsp1 from the *cam1* promoter are long and bent and detached from the SPB, a phenomenon also observed in cells lacking Mto1 (Figure 6A, bottom panel). Quantification data showed that the distribution patterns of microtubule bundle number are similar in *mto1*Δ and P_{cam1}-Rsp1-GFP cells (Figure 6C). Furthermore, direct visualization of Mto1-3GFP in cells expressing Rsp1 from the *cam1* promoter revealed defective localization of Mto1 to all MTOCs (Figure 6D).

We further tested whether such impairment of Mto1 localization to microtubules by Rsp1 overexpression could affect the activity of Mto1 in activating microtubule nucleation. We performed coimmunoprecipitation experiments to analyze the binding between Mto1 and Alp4, the γ-TuSC component. The results showed that the amount of Alp4 that bound Mto1 significantly decreased in cells overexpressing Rsp1 (Figure 6, E and F), suggesting that the sustained interaction between Rsp1 and Mto1 by Rsp1 overexpression most likely attenuates the activity of Mto1 in activating microtubule nucleation. Taken together, these results support the idea that Rsp1 promotes Mto1 redistribution to organize microtubule assembly within the cell.

DISCUSSION

In the present work, we demonstrate that the J-domain cochaperone Rsp1 ensures proper interphase microtubule organization by regulating the distribution of Mto1 among multiple MTOCs (Figure 7). Our work identifies Rsp1 as a new regulatory protein of Mto1 (Figure 2). The two proteins physically interact (Figure 5, A–D), and the interaction is required for the proper localization of Mto1 to the iMTOCs on preexisting microtubules (Figure 5, G and H) and for non-SPB microtubule assembly on preexisting microtubules (Figure 1).

It has been shown that Mto1 and Mto2 form higher-order structures to recruit γ-TuRC to multiple MTOCs and activate γ-TuRC–mediated microtubule nucleation (Lynch *et al.*, 2014). Owing to the limited availability of free Mto1 (Lynch *et al.*, 2014), the SPB and the multiple iMTOCs, both on the nuclear envelope and on preexisting microtubules, must compete for Mto1. Therefore, it is conceivable that promoting Mto1 redistribution will greatly enhance the ability of a cell to supply Mto1 for new microtubule nucleation. Our current work shows that the absence of the J-domain cochaperone Rsp1 results in impaired localization of Mto1 to the iMTOCs on microtubules and drastic Mto1 accumulation at the SPB and the

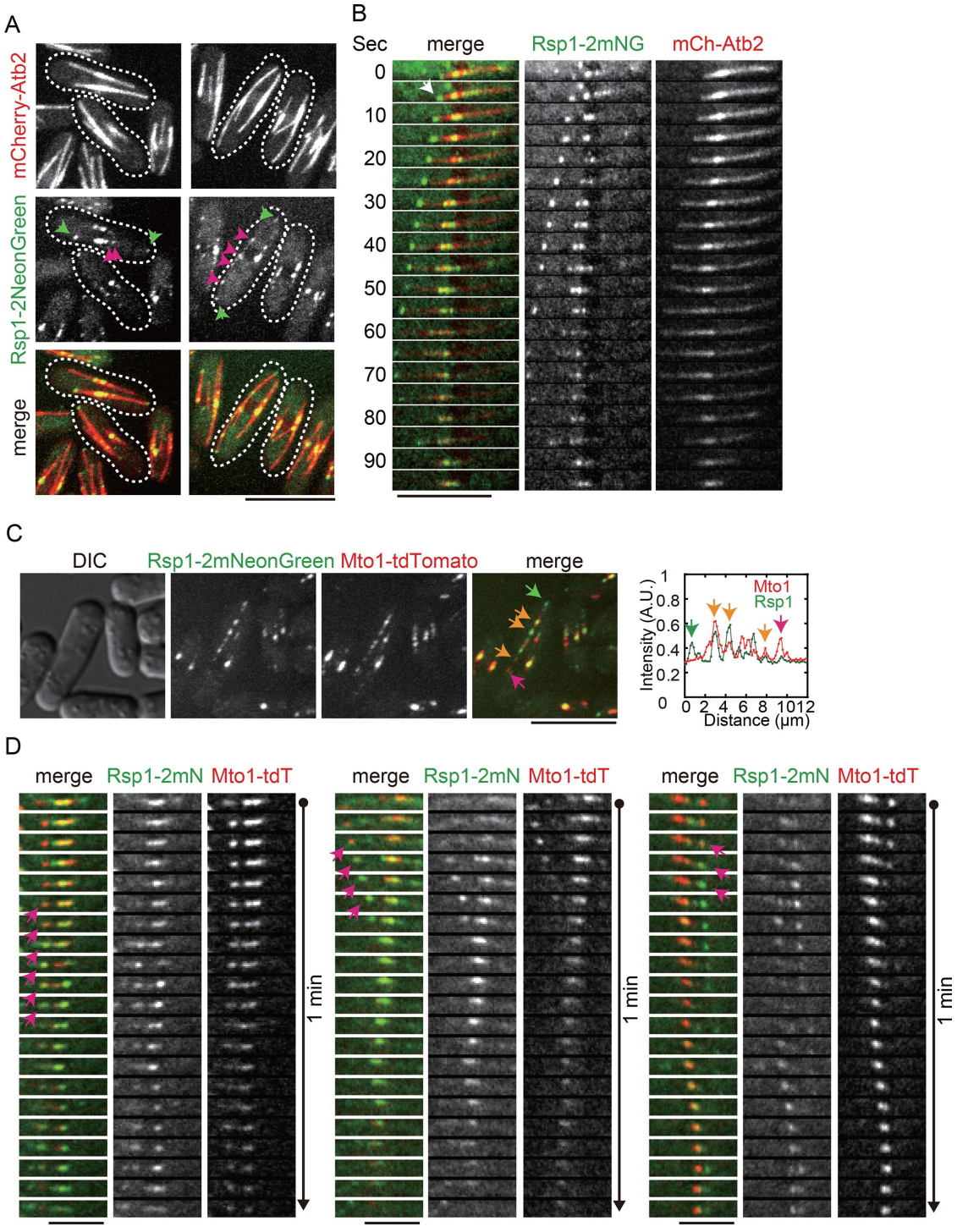

FIGURE 4: Endogenous localization and dynamics of Rsp1. (A) Maximum projection images of WT cells expressing Rsp1-2mNeonGreen and mCherry-Atb2. Rsp1 localized to microtubule plus ends (green arrowheads) and on microtubules (pink arrowheads). Scale bar: 10 μm. (B) Maximum projection time-lapse images of a microtubule (marked by mCherry-Atb2) and Rsp1-2mNeonGreen. The microtubule plus end is indicated by a white arrow. Scale bar: 10 μm. (C) Maximum projection images of WT cells expressing Rsp1-2mNeonGreen and Mto1-tdTomato. Line-scan fluorescence intensity measurements showed that not all Rsp1 colocalized with Mto1-tdTomato. The yellow arrows indicate colocalization of the two proteins, while the green and pink arrows mark those that do not colocalize. Scale bar: 10 μm. (D) Maximum projection time-lapse images of WT cells expressing Rsp1-2mNeonGreen and Mto1-tdTomato. Pink arrows mark colocalization of Rsp1 and Mto1. Scale bar: 10 μm.

nuclear envelope and causes a great reduction of non-SPB microtubules on preexisting microtubules (Figures 1 and 2A). We interpret these data as evidence that Rsp1 is a key player in promoting Mto1 redistribution for regulating non-SPB microtubule organization. Mechanistically, we speculate that Rsp1 may act by promoting Mto1 disassembly/turnover at the multiple MTOCs, particularly at

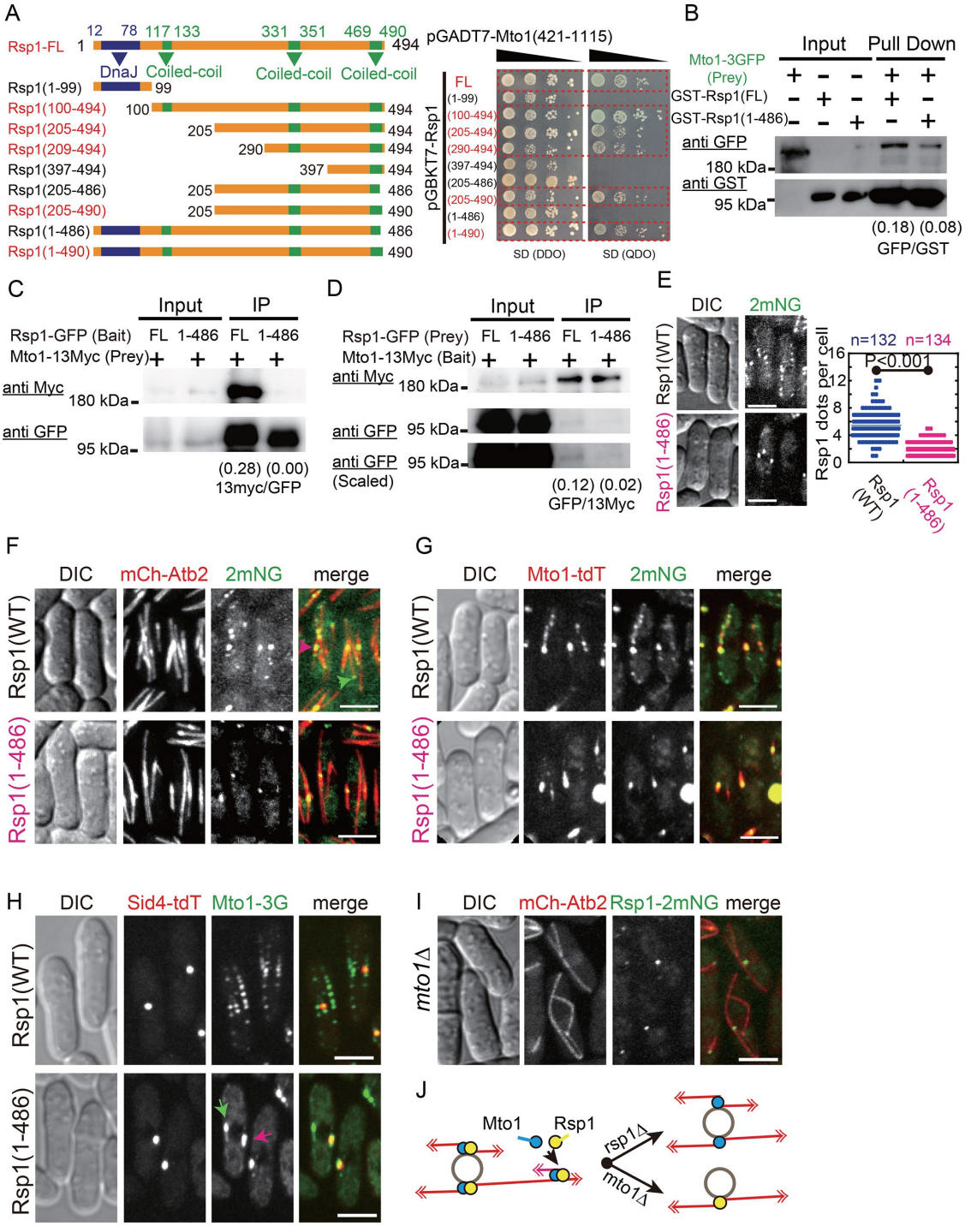

FIGURE 5: Rsp1 interacts with Mto1. (A) Domain structure of Rsp1 and the deletion truncation mutants of Rsp1 used in the yeast-two-hybrid assays. Y2Gold budding yeast cells containing the indicated plasmids were grown on SD DDO (SD/-Leu/-Trp) and QDO (SD/-Ade/-Ura/-Leu/-Trp plus X-α-Gal and aureobasidin A) plates. The numbers in parentheses indicate amino acid positions. Note that the Rsp1 deletion truncation mutants lacking amino acid residues 487–494 do not interact with Mto1(421-1115) and that the residues 290–396 in Rsp1 are also required for interacting with Mto1(421-1115). (B) GST pull-down assays with the recombinant proteins GST-Rsp1 (full length) and GST-Rsp1(1-486) and cell lysate containing Mto1-3GFP. Western blot analysis was performed with antibodies against GFP and GST (also see the full membranes in Supplemental Figure S3A). The ratio of GFP/GST intensity is shown in parentheses. Note that the interaction between GST-Rsp1(1-486) and Mto1-3GFP was impaired. (C, D) Coimmunoprecipitation assays with cells expressing Mto1-13Myc and either Rsp1-GFP or Rsp1(1-486)-GFP. Anti-GFP (C) or anti-Myc (D) antibody-bound protein G beads were incubated with the cell lysate, and Western blot analysis was carried out with antibodies against GFP and Myc (also see the full membranes in Supplemental Figure S3, B and C). The ratio of Myc/GFP intensity is shown in parentheses. (E) Maximum projection images of Rsp1-2mNeonGreen and Rsp1(1-486)-2mNeonGreen expressing cells. Rsp1(1-486) failed to localize along microtubules, and quantification of Rsp1-2mNeonGreen and

the SPB and the iMTOCs on the nuclear envelope. This idea is consistent with the findings that J-domain proteins are able to dismantle higher-order protein structures, including the clathrin cage (Xing *et al.*, 2010; Rothnie *et al.*, 2011) and the spliceosome (Sahi *et al.*, 2010). Canonically, J-domain proteins work as cochaperones to enhance the ATPase activity of Hsp70 and, together with Hsp70, function to facilitate refolding of unfolded proteins, to prevent protein aggregation, and to control the stability and activity of their client proteins (Kampinga and Craig, 2010; Ajit Tamadaddi and Sahi, 2016). Our idea that Rsp1 promotes Mto1 disassembly/turnover is also consistent with the finding that Rsp1 is require to disassemble the equatorial PAA microtubules (Zimmerman *et al.*, 2004), the formation of which depends on the Mto1-Mto2 complex (Sawin *et al.*, 2004; Samejima *et al.*, 2005; Lynch *et al.*, 2014). Furthermore, the *rsp1-1* mutant that is defective in interacting with Hsp70/Ssa1 displays disorganized interphase microtubule arrays (Zimmerman *et al.*, 2004). It is therefore conceivable that Rsp1 works in concert with Hsp70/Ssa1 to regulate Mto1 for proper interphase microtubule organization. Other mechanisms of Rsp1 for regulating Mto1 are possible. These include the following: 1) Rsp1 regulates the affinity of Mto1 to microtubules by the microtubule targeting mechanism reported previously (Samejima *et al.*, 2010); 2) Rsp1 functions as a size-controller of Mto1 by a mechanism yet unknown; and 3) Rsp1 interacts with Mto1 to regulate its activity, which is required for microtubule nucleation, as reported previously (Samejima *et al.*, 2008) (also see Figure 6, D–F). These possibilities await further investigation.

Mto1 preferentially accumulates at the SPB and the iMTOCs on the nuclear envelope, but not at the iMTOCs on preexisting microtubules, in cells lacking Rsp1 or expressing Rsp1(1-486) (Figures 2A and 5H and Supplemental Figure S2D). This preferential accumulation indicates that Mto1 may have a higher affinity to the SPB and the iMTOCs on the nuclear envelope than the iMTOCs on microtubules. Alternatively, Mto1 may preferentially associate with the adaptor proteins at the SPB and the iMTOCs on the nuclear envelope, but not the iMTOCs on preexisting microtubules. However, the respective adaptor proteins have not been identified, despite the fact that Sid4p and Cdc11p, the SPB proteins responsible for recruiting the septation initiation network components, have been shown to be required for Mto1 localization to the SPBs during mitosis, but not during interphase (Samejima *et al.*, 2010). Intriguingly, Mto1 aggregates in anucleate cells lacking Rsp1 (Figure 3). This result underscores the nature of Mto1 to form higher-order structures in an SPB/nucleus-independent manner and highlights the crucial role of Rsp1 in disassembling Mto1 aggregates.

Non-SPB microtubule biogenesis appears to be important in maintaining dynamic microtubule overlapping regions adjacent to the nucleus (Figure 1, A and F). The physiological significance of such dynamic structures is unclear, but our work clearly suggests that Rsp1 is a critical player in maintaining these structures. Without Rsp1, microtubule overlapping regions are short and stable, which is in a sharp contrast to the dynamic microtubule overlapping regions in WT cells (Figure 1F). Presumably, the abnormal stability of microtubule overlapping regions in cells lacking Rsp1 is caused by Mto1 accumulation at the SPB and the nuclear envelope iMTOCs (Figure 2A). Therefore, Rsp1 is also a key player in organizing overall microtubule structures within the cell.

In addition to promoting Mto1 redistribution, Rsp1 may have extra complex functions, because Rsp1 localizes not only on microtubules but also at microtubule plus ends (Figure 4, A–C). The localization of Rsp1 to the microtubule surface supports the role of Rsp1 in promoting non-SPB microtubule formation. However, the role of Rsp1 at microtubule plus ends is still unknown. We speculate that Rsp1 at microtubule plus ends could functionally and/or physically associate with unidentified proteins to orchestrate microtubule dynamics. This awaits further investigation.

Mto1 belongs to the CM1 motif protein family that is conserved through evolution. Proteins in this family function similarly to recruit and activate γ-TuRC (Wu and Akhmanova, 2017). By contrast, the counterparts of the J-domain cochaperone Rsp1 in mammals have not been identified. Nevertheless, a large number of J-domain cochaperones are present in mammalian cells (Kampinga and Craig, 2010; Ajit Tamadaddi and Sahi, 2016). Given this and the conservative nature of Mto1, we expect that the distribution of Mto1 counterparts/homologues in higher eukaryotic cells may be regulated by a similar J-domain cochaperone-dependent mechanism. This merits further investigation.

In conclusion, we demonstrated that Rsp1 specifies the localization of Mto1 to noncentrosomal microtubules to orchestrate their cellular dynamics. Our findings provide novel insights into the function and molecular mechanism of Rsp1-Mto1 interaction in spatial control of the microtubule network and plasticity in eukaryotic cells.

MATERIALS AND METHODS

Yeast genetics

Yeast strains were created either by random spore digestion or by tetrad dissection, as described previously (Forsburg and Rhind, 2006). Gene deletion and tagging were performed by the PCR-based method using the pFA6a series of plasmids (Hentges *et al.*, 2005), and yeast transformation was carried out by the lithium acetate method. Culture media were purchased from Formedium (www.formedium.com), and the drugs G418, nourseothricin, and hygromycin B were purchased from Formedium, Werner Bioagents (www.webioage.de), and Sigma Aldrich (www.sigmaaldrich.com), respectively. For live-cell imaging, cells were cultured in Edinburgh minimal medium supplied with adenine, leucine, uracil, histidine,

Rsp1(1-486)-2mNeonGreen dots within the cells showed that Rsp1 dot number decreased significantly in the mutant cells. The *p* value was calculated by Wilcoxon–Mann–Whitney test, and *n* indicates cell number. Scale bar: 5 μm. (F) Maximum projection images of cells expressing mCherry-Atb2 and either Rsp1-2mNeonGreen or Rsp1(1-486)-2mNeonGreen. Pink and green arrowheads mark Rsp1 on microtubules and at the microtubule plus end. The microtubule localization of Rsp1(1-486)-2mNeonGreen was impaired. Scale bar: 5 μm. (G) Maximum projection images of cells expressing Mto1-tdTomato and either Rsp1-2mNeonGreen or Rsp1(1-486)-2mNeonGreen. Scale bar: 5 μm. (H) Maximum projection images of Rsp1 and Rsp1(1-486) cells expressing Sid4-tdTomato and Mto1-3GFP. Rsp1(1-486) caused Mto1-3GFP concentration at the SPB (pink arrow) and/or the nuclear envelope iMTOC(s) (green arrow). Scale bar: 5 μm. (I) Maximum projection images of *mto1*Δ cells expressing Rsp1-2mNeonGreen and mCherry-Atb2. Note that Rsp1-2mNeonGreen localized to only the SPB in the absence of Mto1. Scale bar: 5 μm. (J) Diagram illustrating the localization relationship between Rsp1 and Mto1. Both proteins localize on microtubules in an interdependent manner but localize to the SPB in an independent manner.

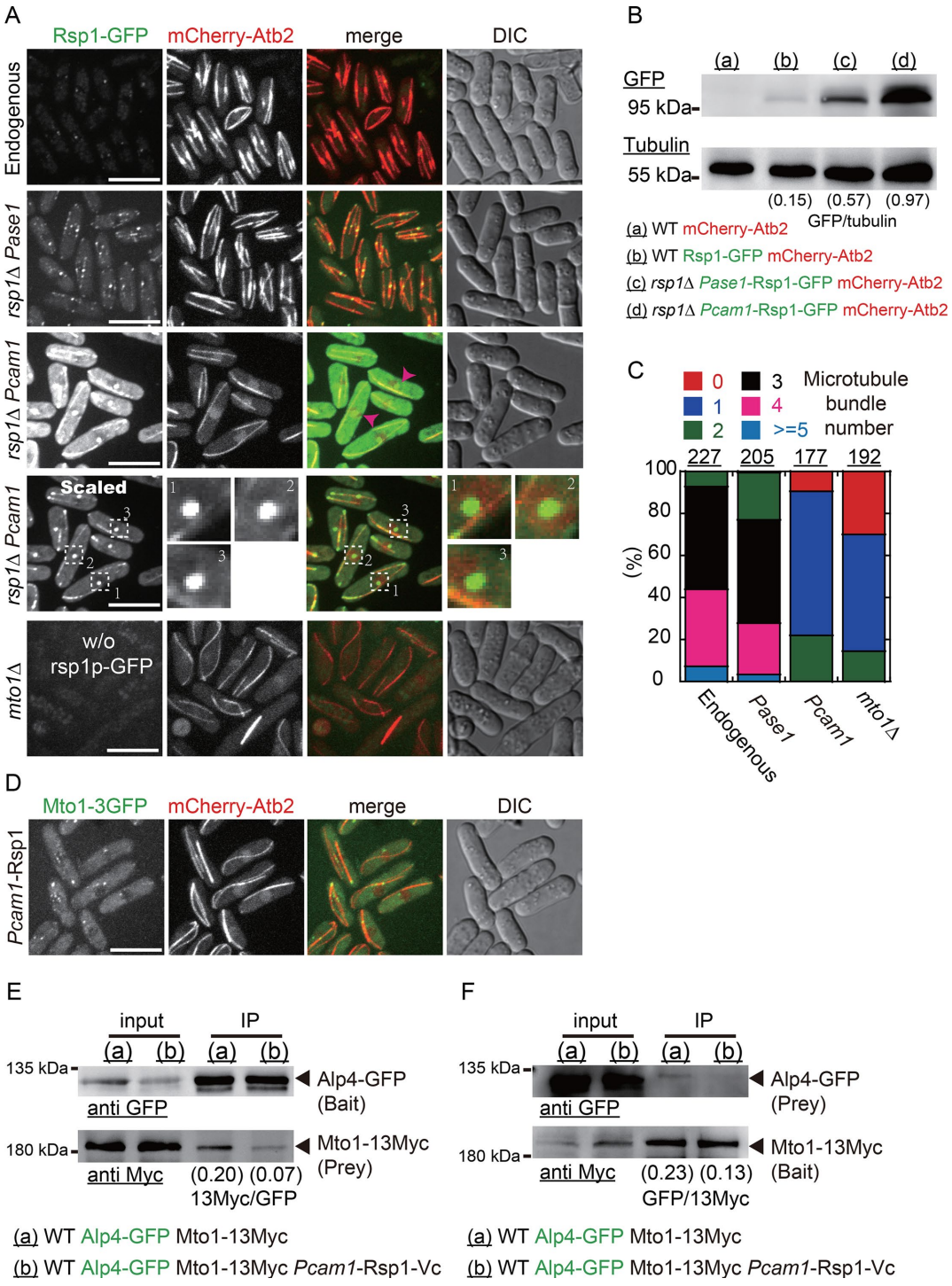

FIGURE 6: Rsp1 overexpression results in defective microtubule localization of Mto1-3GFP and reduces microtubule number. (A) Maximum projection images of WT and *rsp1*Δ cells expressing mCherry-Atb2 and either endogenous Rsp1-GFP or Rsp1-GFP from the *ase1* promoter (P_{ase1}) and the *cam1* promoter (P_{cam1}). The bottom panel shows *mto1*Δ cells expressing only mCherry-Atb2. Overexpression of Rsp1 reduced microtubules number and appeared to detach microtubules from the SPB (marked by pink arrowheads and highlighted in the *Pcam1*-Rsp1–expressing cells 1, 2, and 3), a phenotype also observed in *mto1*Δ cells. Note that all images were scaled consistently for comparison, except the one indicated as "Scaled," which was scaled to display the saturated GFP signals. Scale bar: 10 μm. (B) Western blot analysis of Rsp1-GFP expression in the indicated cells (also see the full membranes in Supplemental Figure S4A). The ratio of GFP/tubulin intensity is shown in parentheses. (C) Quantification of microtubule bundle number for the cells in A. Rsp1-overexpressing and *Mto1*Δ cells give similar distribution patterns of the quantification. (D) Maximum projection images of *Pcam1*-Rsp1 cells expressing Mto1-3GFP and mCherry-Atb2. The microtubule localization of Mto1 was impaired. Scale bar: 10 μm. (E, F) Coimmunoprecipitation of Mto1-13Myc and Alp4-GFP. GFP (E) or Myc (F) antibody-bound protein G beads were used for the coimmunoprecipitation experiments, and Western blot analysis was carried out with antibodies against GFP and Myc (see also the full membranes in Supplemental Figure S4, B and C). The ratio of Myc/GFP intensity is shown in parentheses.

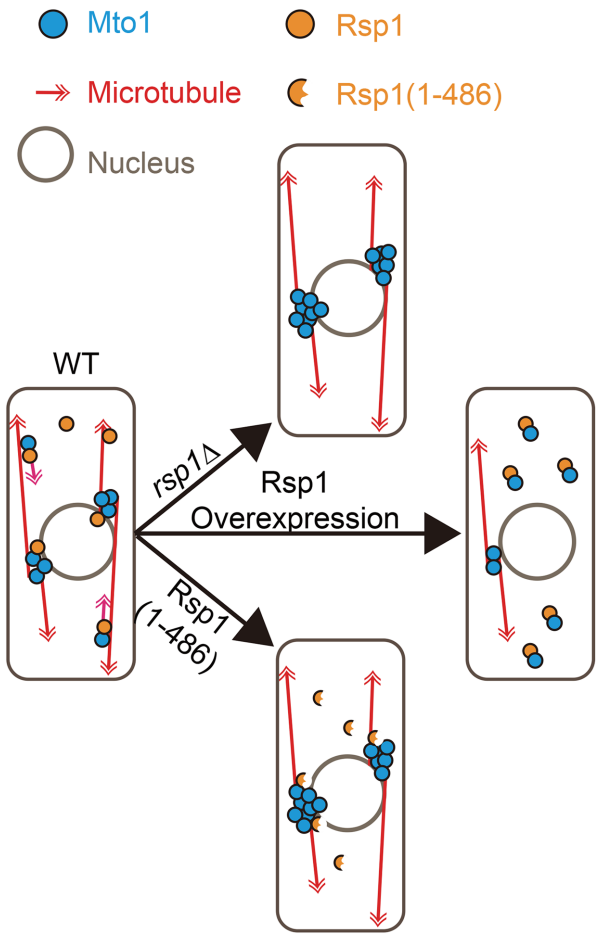

FIGURE 7: Working model of Rsp1 regulation of Mto1. Diagrams illustrate coordination of Rsp1 and Mto1 in regulating non-SPB microtubule assembly. In WT cells, the proper localization of Mto1 at the iMTOCs along microtubule bundles requires Rsp1. In cells lacking Rsp1 (*rsp1*Δ) or expressing Rsp1(1-486) that does not interact with Mto1, Mto1 accumulates at the SPB and/or the iMTOC on the nuclear envelope. Rsp1 overexpression compromises the localization of Mto1 to all MTOCs, including the SPB. We propose that Rsp1 functions to promote the redistribution of Mto1 at the multiple MTOCs (the SPB, iMTOCs on microtubule bundles, and iMTOCs on the nuclear envelope) for proper microtubule organization.

and lysine (0.225 g/l each), and for biochemistry, cells were cultured in yeast extract (YE) medium containing the five supplements. The yeast strains used in this study are listed in Supplemental Table S1.

Molecular cloning

Cloning was performed with enzymes purchased from NEB (www.neb.com), and the QuikChange II XL Site-Directed mutagenesis kit was used to generate mutations (www.agilent.com). All plasmids used in this study are listed in Supplemental Table S2.

Yeast two-hybrid assays

For yeast two-hybrid assays, the Matchmaker Gold Yeast Two-Hybrid System was used (www.clontech.com). Briefly, the indicated Mto1 truncation mutant was cloned into the pGADT7 vector and full-length Rsp1 and its truncation mutants were cloned into the pGBKT7 vector. The interaction between Mto1 and Rsp1 was then tested by transforming the pGADT7 and pGBKT7 plasmids into Y2H gold budding yeast cells grown on SD/-Leu/-Trp dropout (double-dropout [DDO]) plates and SD/-Ade/-His/-Leu/-Trp dropout (quadruple-dropout [QDO]) plates containing aureobasidin A and X-a-Gal.

Biochemistry

Recombinant GST fusion proteins were produced in *Escherichia coli* BL21 or Rosetta cells and were purified with glutathione Sepharose 4B resins (www.gelifesciences.com). For GST pull-down assays, glutathione Sepharose 4B resins with immobilized GST fusion proteins were incubated with precleaned yeast cell lysate, prepared by liquid nitrogen grinding with a mortar grinder RM 200 (www.retsch.com), in TBS buffer containing 0.1% Triton X-100 and cocktail protease inhibitors for 2 h at 4°C, and the resins were then washed with the TBS+0.1% Triton X-100 buffer five times and with TBS buffer one time. Finally, the glutathione Sepharose 4B resins were boiled in SDS sample buffer for further SDS–PAGE and Western blot analysis. Similarly, coimmunoprecipitation assays were performed with Dynabeads protein G beads (www.thermofisher.com) and strains expressing the indicated GFP and 13Myc proteins in TBS plus 0.1% Triton X-100. Immunoprecipitated proteins were then analyzed by Western blotting with antibodies against GFP (www.rockland-inc.com) and myc (www.rockland-inc.com). For testing protein expression levels, cells in the exponential phase were collected, and protein extract was prepared using the NaOH method, as previously described (Matsuo *et al.*, 2006). Protein extract was then analyzed by Western blotting with antibodies against GFP and tubulin (www.enogene.com).

Preparation of anucleate cells

Anucleate cells were generated by centrifugation with an Optima MAX-XP tabletop ultracentrifuge equipped with a TLA-100 rotor (www.beckmancoulter.com). Briefly, cells in the exponential phase were centrifuged at 25,000 rpm for 10 min at 4°C, and the cells were then suspended in fresh YE medium and recultured at 30°C for 10–20 min before microscopic observation.

Microscopy and data analysis

Live-cell microscopic experiments were carried out with a Perkin-Elmer UltraVIEW VoX spinning-disk microscope equipped with a Hamamatsu C9100-23B EMCCD camera and a CFI Apochromat TIRF 100× objective (NA = 1.49). Imaging was performed using agarose-pad slides at room temperature, as described previously (Tran *et al.*, 2004). For maximum projection imaging, stack images containing 11 planes with 0.5-μm spacing were acquired; for high-temporal-resolution imaging, single-plane images were acquired. MetaMorph v. 7.7 software (www.moleculardevices.com), together with ImageJ v. 1.5 (imagej.nih.gov), was used to analyze microscopic data, to create the kymograph graphs, and to perform the fluorescence intensity measurements. Plot graphs were generated with KaleidaGraph v. 4.5 (www.synergy.com), and statistical analysis was performed with either Microsoft Excel or KaleidaGraph.

ACKNOWLEDGMENTS

We thank Quanwen Jin (Xiamen University), Phong Tran (University of Pennsylvania), Dannel McCollum (University of Massachusetts), Fred Chang (Columbia University), and the Yeast Genetic Resource Center Japan for providing yeast strains and plasmids. We thank Quanwen Jin for his critical reading of the paper. This work is supported by the National Natural Science Foundation of China (31671406, 31621002, 91754106, and 31601095), the Strategic Priority Research Program of the Chinese Academy of Sciences

(XDB19040101), and the National Key Research and Development Program of China (2017YFA0503600). C.F. gratefully acknowledges China's 1000 Young Talents Recruitment Program and the Major/Innovative Program of Development Foundation of Hefei Center for Physical Science and Technology (2017FXCX008).

REFERENCES

Ajit Tamadaddi C, Sahi C (2016). J domain independent functions of J proteins. Cell Stress Chaperones 21, 563–570.

Anders A, Lourenco PC, Sawin KE (2006). Noncore components of the fission yeast gamma-tubulin complex. Mol Biol Cell 17, 5075–5093.

Bratman SV, Chang F (2008). Mechanisms for maintaining microtubule bundles. Trends Cell Biol 18, 580–586.

Choi YK, Liu P, Sze SK, Dai C, Qi RZ (2010). CDK5RAP2 stimulates microtubule nucleation by the gamma-tubulin ring complex. J Cell Biol 191, 1089–1095.

Dhani DK, Goult BT, George GM, Rogerson DT, Bitton DA, Miller CJ, Schwabe JW, Tanaka K (2013). Mzt1/Tam4, a fission yeast MOZART1 homologue, is an essential component of the gamma-tubulin complex and directly interacts with GCP3(Alp6). Mol Biol Cell 24, 3337–3349.

Drummond DR, Cross RA (2000). Dynamics of interphase microtubules in *Schizosaccharomyces pombe*. Curr Biol 10, 766–775.

Fong KW, Choi YK, Rattner JB, Qi RZ (2008). CDK5RAP2 is a pericentriolar protein that functions in centrosomal attachment of the gamma-tubulin ring complex. Mol Biol Cell 19, 115–125.

Forsburg SL, Rhind N (2006). Basic methods for fission yeast. Yeast 23, 173–183.

Fujita A, Vardy L, Garcia MA, Toda T (2002). A fourth component of the fission yeast gamma-tubulin complex, Alp16, is required for cytoplasmic microtubule integrity and becomes indispensable when gamma-tubulin function is compromised. Mol Biol Cell 13, 2360–2373.

Hagan IM (1998). The fission yeast microtubule cytoskeleton. J Cell Sci 111, 1603–1612.

Hagan IM, Hyams JS (1988). The use of cell division cycle mutants to investigate the control of microtubule distribution in the fission yeast *Schizosaccharomyces pombe*. J Cell Sci 89, 343–357.

Hamill DR, Severson AF, Carter JC, Bowerman B (2002). Centrosome maturation and mitotic spindle assembly in *C. elegans* require SPD-5, a protein with multiple coiled-coil domains. Dev Cell 3, 673–684.

Hanafusa H, Kedashiro S, Tezuka M, Funatsu M, Usami S, Toyoshima F, Matsumoto K (2015). PLK1-dependent activation of LRRK1 regulates spindle orientation by phosphorylating CDK5RAP2. Nat Cell Biol 17, 1024–1035.

Hentges P, Van Driessche B, Tafforeau L, Vandenhaute J, Carr AM (2005). Three novel antibiotic marker cassettes for gene disruption and marker switching in *Schizosaccharomyces pombe*. Yeast 22, 1013–1019.

Hoog JL, Schwartz C, Noon AT, O'Toole ET, Mastronarde DN, McIntosh JR, Antony C (2007). Organization of interphase microtubules in fission yeast analyzed by electron tomography. Dev Cell 12, 349–361.

Horio T, Uzawa S, Jung MK, Oakley BR, Tanaka K, Yanagida M (1991). The fission yeast gamma-tubulin is essential for mitosis and is localized at microtubule organizing centers. J Cell Sci 99, 693–700.

Janson ME, Loughlin R, Loiodice I, Fu C, Brunner D, Nedelec FJ, Tran PT (2007). Crosslinkers and motors organize dynamic microtubules to form stable bipolar arrays in fission yeast. Cell 128, 357–368.

Kampinga HH, Craig EA (2010). The HSP70 chaperone machinery: J proteins as drivers of functional specificity. Nat Rev Mol Cell Biol 11, 579–592.

Knop M, Schiebel E (1998). Receptors determine the cellular localization of a gamma-tubulin complex and thereby the site of microtubule formation. EMBO J 17, 3952–3967.

Lin TC, Neuner A, Schiebel E (2015). Targeting of gamma-tubulin complexes to microtubule organizing centers: conservation and divergence. Trends Cell Biol 25, 296–307.

Loiodice I, Staub J, Setty TG, Nguyen NP, Paoletti A, Tran PT (2005). Ase1p organizes antiparallel microtubule arrays during interphase and mitosis in fission yeast. Mol Biol Cell 16, 1756–1768.

Lynch EM, Groocock LM, Borek WE, Sawin KE (2014). Activation of the gamma-tubulin complex by the Mto1/2 complex. Curr Biol 24, 896–903.

Masuda H, Mori R, Yukawa M, Toda T (2013). Fission yeast MOZART1/Mzt1 is an essential gamma-tubulin complex component required for complex recruitment to the microtubule organizing center, but not its assembly. Mol Biol Cell 24, 2894–2906.

Matsuo Y, Asakawa K, Toda T, Katayama S (2006). A rapid method for protein extraction from fission yeast. Biosci Biotechnol Biochem 70, 1992–1994.

Oakley BR, Paolillo V, Zheng Y (2015). γ-Tubulin complexes in microtubule nucleation and beyond. Mol Biol Cell 26, 2957–2962.

Petry S, Vale RD (2015). Microtubule nucleation at the centrosome and beyond. Nat Cell Biol 17, 1089–1093.

Roostalu J, Surrey T (2017). Microtubule nucleation: beyond the template. Nat Rev Mol Cell Biol 18, 702–710.

Rothnie A, Clarke AR, Kuzmic P, Cameron A, Smith CJ (2011). A sequential mechanism for clathrin cage disassembly by 70-kDa heat-shock cognate protein (Hsc70) and auxilin. Proc Natl Acad Sci USA 108, 6927–6932.

Sagolla MJ, Uzawa S, Cande WZ (2003). Individual microtubule dynamics contribute to the function of mitotic and cytoplasmic arrays in fission yeast. J Cell Sci 116, 4891–4903.

Sahi C, Lee T, Inada M, Pleiss JA, Craig EA (2010). Cwc23, an essential J protein critical for pre-mRNA splicing with a dispensable J domain. Mol Cell Biol 30, 33–42.

Samejima I, Lourenco PC, Snaith HA, Sawin KE (2005). Fission yeast mto2p regulates microtubule nucleation by the centrosomin-related protein mto1p. Mol Biol Cell 16, 3040–3051.

Samejima I, Miller VJ, Groocock LM, Sawin KE (2008). Two distinct regions of Mto1 are required for normal microtubule nucleation and efficient association with the gamma-tubulin complex in vivo. J Cell Sci 121, 3971–3980.

Samejima I, Miller VJ, Rincon SA, Sawin KE (2010). Fission yeast Mto1 regulates diversity of cytoplasmic microtubule organizing centers. Curr Biol 20, 1959–1965.

Sawin KE, Lourenco PC, Snaith HA (2004). Microtubule nucleation at non-spindle pole body microtubule-organizing centers requires fission yeast centrosomin-related protein mod20p. Curr Biol 14, 763–775.

Sawin KE, Tran PT (2006). Cytoplasmic microtubule organization in fission yeast. Yeast 23, 1001–1014.

Shaner NC, Lambert GG, Chammas A, Ni Y, Cranfill PJ, Baird MA, Sell BR, Allen JR, Day RN, Israelsson M, *et al*. (2013). A bright monomeric green fluorescent protein derived from *Branchiostoma lanceolatum*. Nat Methods 10, 407–409.

Terada Y, Uetake Y, Kuriyama R (2003). Interaction of Aurora-A and centrosomin at the microtubule-nucleating site in *Drosophila* and mammalian cells. J Cell Biol 162, 757–763.

Tran PT, Paoletti A, Chang F (2004). Imaging green fluorescent protein fusions in living fission yeast cells. Methods 33, 220–225.

Usui T, Maekawa H, Pereira G, Schiebel E (2003). The XMAP215 homologue Stu2 at yeast spindle pole bodies regulates microtubule dynamics and anchorage. EMBO J 22, 4779–4793.

Woodruff JB, Ferreira Gomes B, Widlund PO, Mahamid J, Honigmann A, Hyman AA (2017). The centrosome is a selective condensate that nucleates microtubules by concentrating tubulin. Cell 169, 1066–1077 e1010.

Wu J, Akhmanova A (2017). Microtubule-organizing centers. Annu Rev Cell Dev Biol 33, 51–75.

Xia P, Zhou J, Song X, Wu B, Liu X, Li D, Zhang S, Wang Z, Yu H, Ward T, *et al*. (2014). Aurora A orchestrates entosis by regulating a dynamic MCAK-TIP150 interaction. J Mol Cell Biol 6, 240–254.

Xing Y, Bocking T, Wolf M, Grigorieff N, Kirchhausen T, Harrison SC (2010). Structure of clathrin coat with bound Hsc70 and auxilin: mechanism of Hsc70-facilitated disassembly. EMBO J 29, 655–665.

Yamashita A, Sato M, Fujita A, Yamamoto M, Toda T (2005). The roles of fission yeast ase1 in mitotic cell division, meiotic nuclear oscillation, cytokinesis checkpoint signaling. Mol Biol Cell 16, 1378–1395.

Zimmerman S, Chang F (2005). Effects of γ-tubulin complex proteins on microtubule nucleation and catastrophe in fission yeast. Mol Biol Cell 16, 2719–2733.

Zimmerman S, Tran PT, Daga RR, Niwa O, Chang F (2004). Rsp1p, a J domain protein required for disassembly and assembly of microtubule organizing centers during the fission yeast cell cycle. Dev Cell 6, 497–509.